Materials Science & Engineering C 81 (2017) 588–596

Contents lists available at ScienceDirect

Materials Science & Engineering C

journal homepage: www.elsevier.com/locate/msec

Development and evaluation of thymol-chitosan hydrogels with antimicrobial-antioxidant activity for oral local delivery

María Inés Alvarez Echazú[a], Christian Ezequiel Olivetti[a], Claudia Anesini[a], Claudio Javier Perez[b], Gisela Solange Alvarez[a], Martin Federico Desimone[a,*]

[a] Universidad de Buenos Aires, Consejo Nacional de Investigaciones Científicas y Técnicas (CONICET), Instituto de Química y Metabolismo del Fármaco (IQUIMEFA), Facultad de Farmacia y Bioquímica, Junín 956, Piso 3° (1113), Buenos Aires, Argentina

[b] Instituto de Investigaciones en Ciencia y Tecnología de Materiales (INTEMA), Grupo Ciencia y Tecnología de Polímeros, Universidad Nacional de Mar del Plata, Juan B. Justo 4302, (7600) Mar del Plata, Argentina

ABSTRACT

Nowadays, the research of innovative drug delivery devices is focused on the design of multiple drug delivery systems, the prevention of drug side effects and the reduction of dosing intervals. Particularly, new mucosal delivery systems for antimicrobials, antioxidants and anti-inflammatory drugs has a growing development, regards to the avoidance of side effects, easy administration and a suitable drug concentration in the mucosa. In this work, chitosan hydrogels are evaluated as a biodegradable scaffold and as a bioactive agent carrier of an antioxidant-antimicrobial compound called thymol.

Throughout the study, swelling behavior, viscoelastic properties and thermal analysis are highlighted to present its advantages for a biomedical application. Furthermore, the *in vitro* results obtained indicate that thymol-chitosan hydrogels are biocompatible when exposed to [3T3] fibroblasts, exhibit antimicrobial activity against *Staphylococcus aureus* and *Streptococcus mutans* for 72 h and antioxidant activity for 24 h. These are desirable properties for a mucosal delivery system for an antimicrobial-antioxidant dual therapy for periodontal disease.

1. Introduction

Today, the development of innovative drug delivery devices is centered in the design of multiple drug delivery systems [1,2], the prevention of drug side effects and the reduction of dosing intervals [3]. Accordingly, one strategy to avoid side effects is the development of local delivery systems [4–7]. Thus, dermal, mucosal, ocular and inhalation administration sometimes help to prevent them [8–10].

Particularly, there are some characteristics of the mucous membrane that influence the design of new mucosal delivery systems. The mucous membranes do not possess a keratinized outer layer as the skin and are therefore much more sensitive to irritants. However, they have a good permeability profile, making them a suitable site for drug delivery.

Additionally, the oral cavity is an environment with a high percentage of moisture with natural secretions like saliva that tend to dilute drugs, so that to achieve a continuous action, multiple applications are required.

Furthermore, usually diseases imply complex and diverse mechanisms in which are needed a variety of molecules to achieve a suitable treatment. Periodontal disease is an example. Bacteria that cause periodontal tissue destruction and inflammation are present throughout every stage of the disease [11,12]. Therefore, antimicrobials, antioxidants, anti-resorptives and anti-inflammatory drugs are required along the treatment [13–18].

Nowadays, some commercial products for periodontal disease include mouthwashes which are applied daily, systemic antibiotics and devices for local delivery of bioactives [19,20].

Taking this into account, thymol has promising characteristics for oral therapy. It has antimicrobial [21–23] and antioxidant properties [24] as well as suitable organoleptic characteristics for oral delivery. Nevertheless, it is slightly soluble in water and volatile. These disadvantages are clearly obstacles to develop an oral delivery device.

Chitosan is a linear polysaccharide constituted by glucosamine and *N*-acetyl-glucosamine derived from crustacean shells that has promising features for biomedical applications. Chitosan amine groups can establish ionic interactions while acetamide groups can participate in hydrophobic interactions, leading to a broad spectrum of candidate

* Corresponding author.
E-mail address: desimone@ffyb.uba.ar (M.F. Desimone).

http://dx.doi.org/10.1016/j.msec.2017.08.059
Received 28 April 2017; Received in revised form 31 July 2017; Accepted 10 August 2017
Available online 15 August 2017
0928-4931/

molecules for drug delivery and high adsorption capacities [25].

Moreover, chitosan functional groups such as hydroxyl and amine groups can be chemically modified [26]. The addition of alkyl and carboxymethyl groups to chitosan changes its physical, chemical and mechanical properties [27]. Interestingly, many advances have been accomplished in chemical and enzymatic modifications. In case of enzymatic modifications, they have demonstrated high specificity while using environmentally friendly reaction conditions [28].

Chitosan has also shown antimicrobial activity [29–31]. Nevertheless, some discrepancies are found in literature. Antimicrobial activity is influenced by polymer factors like deacetylation degree and external factors such as type of microorganism and pH. Additionally, there are several hypotheses of chitosan mechanism of action. Some authors postulate chitosan as a chelating agent, others as a polycationic polymer that binds to microorganisms anionic cell surface proteins [32].

Besides, chitosan cytocompatibility was studied in many types of cells (*i.e.*: osteoblasts, fibroblasts, neural cells) [33–35]. Cells can adhere and proliferate in chitosan matrix showing good biocompatibility. Some authors argue that the homology between chitosan biopolymer and native hyaluronic acid or other extracellular glucosamines could be one of the reasons of its biocompatibility [36]. For these reasons, chitosan biopolymer and composites are considered as good candidates for tissue engineering and wound healing [37–39].

Furthermore, chitosan is a biodegradable polymer. Indeed, lysozyme and some proteinases can degrade chitosan into well known and non-toxic products. Biodegradable scaffolds and delivery devices have promising clinical applications, because they usually show good patient compliance and acceptance [40].

Lastly, chitosan is a mucoadhesive polymer [36,41,42]. Mucoadhesion is a process in which chemical interactions are established between the mucin and the biopolymer. The nature of these interactions differs according to the biopolymer characteristics. The mucoadhesion process can be divided in two different events. Firstly, the polymer gets wet and expands into the mucin network. Secondly, covalent, ionic and hydrogen bonds, Van der Waals forces and electrostatic interactions are established between the polymer and the mucin. In the case of chitosan, amine and hydroxyl groups form hydrogen bonds with mucin and also its linear structure gives good flexibility to the polymer encouraging mucoadhesion [43]. In conclusion, chitosan biopolymer has good qualities for the development of drug delivery and tissue regeneration biomaterials [44,45].

Particularly, chitosan hydrogels can be used as carriers for drug release and as a biodegradable scaffold for periodontal tissue regeneration. In periodontal disease therapy, not only it is important to treat signs and symptoms, but also the recovery of lost tissue. Nowadays, the complete recovery of periodontal tissue still seems too far to achieve. Nevertheless, major advances have been carried out in alveolar bone regeneration thanks to ceramic materials such as silica, hydroxyapatite and calcium phosphate [46,47] given that bioactive ceramic materials encourage bone formation [48]. Additionally, there is a growing development in periodontal soft tissue regeneration regards to organic materials like collagen and chitosan [49,50,51].

Herein, a chitosan hydrogel developed by a spraying method with rheological properties, swelling behavior and a porous structure suitable for drug delivery is presented as an alternative for periodontal disease treatment. We promoted sol-gel transition with an alkali solution spray incorporating thymol, an antimicrobial-antioxidant compound in the resulting hydrogels. Cytocompatibility assays with [3T3] mouse fibroblasts were performed confirming its biocompatibility. In addition, the incorporation of thymol into chitosan polymeric network, its release kinetics as well as its antimicrobial and antioxidant activities were tested in the search of a biomaterial that fulfills the requirements of a biomaterial with dual therapy properties for periodontal disease.

2. Experimental

2.1. Reagents and materials

Low-viscosity chitosan obtained from crab shells, structural viscosity 66 mPas, Deacetylation > 75.0%, lysozyme from chicken egg white (100,000 U/mg) and thiazolyl blue tetrazolium bromide reagent, DPPH (2,2-diphenyl-1-picrylhydrazyl), DAB (diaminobencidine tetrahidrochloride) and epinephrine were purchased from Sigma–Aldrich (St Louis, USA). Folin-Ciocalteu's phenol reagent was obtained from Merck (Darmstadt, Germany). Dulbecco's modified Eagle's medium, fetal calf serum, penicillin and streptomycin were purchased from Gibco. Todd-Hewitt broth was obtained from Britania Lab. All other reagents were of analytical grade.

2.2. Chitosan hydrogel synthesis

A 20 $mg \cdot mL^{-1}$ chitosan solution was prepared dissolving the chitosan powder in 1% (v/v) acetic acid. Stirring for almost 15 min was necessary to obtain a homogenous solution. Afterwards, 1 mL of chitosan solution was poured in each well of a 24-well culture plate, used as a template. Then, a 1 N NaOH solution was sprayed on the template and left for 5 h at room temperature. Finally, the NaOH solution was removed and the hydrogels obtained were washed with deionized water until neutral pH was reached.

2.3. Chitosan hydrogel ultrastructural characterization

Chitosan hydrogels were analysed by scanning electron microscopy (SEM). Samples were fixed with a solution of glutaraldehyde (10% *v*/v in PBS) for 1 h at 4 °C. Following fixation, samples were washed three times with PBS and then freezed at − 80 °C. Finally, the samples were freeze-dried and gold sputter-coated for analysis using a Zeiss SUPRA 40 microscope.

Transmission electron microscope (TEM) analysis was performed in a MET Zeiss 109. Following fixation and wash as described above, the samples were post-fixed using a 5% osmium tetra-oxide in a pH 7.4 cacodylate/saccharose buffer (0.05 M/0.3 M) for 1 h at 4 °C. Afterwards, samples were dehydrated and embedded in epoxy resin. Thin sections were cut with an ultra microtome and contrasted by phosphotungstic acid. Recovered sections were imaged using a Zeiss 109 microscope.

2.4. FTIR characterization

Fourier transform infrared (FTIR) spectra from lyophilized chitosan hydrogels were carried out with an FTIR-Raman Thermo Scientific Nicolet model 50 computer IS, which is coupled with an attenuated total reflection device (ATR). Scanning range was 4000–500 cm^{-1}. Spectra was processed by Thermo Nicolet OMNIC software.

2.5. Differential scanning calorimetry (DSC)

Differential scanning calorimetry (DSC) measurements were performed on a Shimadzu DSC-50 instrument. Temperature was calibrated with In (157 °C, 3.3 J mol^{-1}). Approximately 20 mg of the freeze-dried samples were first equilibrated at 25 °C and then heated from 25 to 240 °C at a constant rate of 10 °C min^{-1}, under a nitrogen flow of 50 $mL \cdot min^{-1}$.

2.6. Swelling studies

Chitosan and thymol-chitosan hydrogels were freeze-dried. Afterwards, they were weighted (W_o) and stored in buffer phosphate saline to allow water uptake. Hydrogels were removed from PBS and weighted (W) at different time points (t) after removing the excess of

water. The degree of swelling was calculated by the following equation:

$$W\% = [(W - W_o)/W] \times 100$$

Later, the water content at equilibrium (W_∞) and the kinetic rate constants were calculated according to the next equation:

$$t/W = 1/(KW^2_\infty) + t/W_\infty$$

2.7. Rheological measurements

Chitosan hydrogels rheology was also analysed. Amplitude sweeps were performed first in order to determine the linear viscoelastic range (LVR). The elastic or storage modulus, *G′*, the viscous or loss modulus, *G″* and complex viscosity (η*) of the studied materials were obtained in small-amplitude oscillatory shear flow experiments using a rotational rheometer from Anton Paar (MCR-301) provided with a CTD 600 thermo chamber. The tests were performed using parallel plates of 25 mm diameter, a strain of γ = 1.0% and a frequency range of 0.1–500 s^{-1}. The measurements were carried out at room temperature (20 °C). All the tests were performed using small strains to ensure the linearity of the dynamic responses. All the runs were repeated using different samples. The gap width used was 1.8–2 mm.

2.8. Chitosan biodegradability

Chitosan hydrogels and thymol-loaded chitosan hydrogels were freeze-dried and weighted (W_o). Afterwards, they were immersed in PBS (pH 7.4) with 1 mg·mL^{-1} of lysozyme (100,000 U·mg) at 37 °C. After 7 days, hydrogels were washed, lyophilized and weighted ($W_{7\ days}$). The percentage of weight was assessed to evaluate hydrogel biodegradation according to next equation:

$$W\% = (W_{7\ days}/W_o) \times 100$$

2.9. Cell culture and viability test

[3T3] mouse fibroblast cells were grown in adherent culture flasks with low glucose Dulbecco's modified Eagle's medium (DMEM) supplemented with 10% heat-inactivated fetal calf serum and 1% penicillin–streptomycin. Cells were kept at 37 °C in a humidified 5% carbon dioxide chamber until confluence was reached. Harvesting was done with a trypsin–EDTA solution. Cells were stained with trypan blue and counted with a Neubauer camera. Fibroblast cells (1.22×10^4) were seeded in each hydrogel followed by the addition of 1 mL complete low glucose DMEM medium. After 24 h of incubation at 37 °C, in a 5% CO_2 chamber, cell metabolic activity was measured using the MTT assay. The medium was first removed and replaced by 0.5 mL of a 0.5 mg·mL^{-1} MTT solution in fresh media. Samples were incubated in a humidified 5% carbon dioxide chamber for 4 h. Subsequently, MTT solutions were removed, 1 mL of absolute ethanol was added and the mixtures were incubated for 30 min at room temperature. The absorbance was recorded at 570 nm in a UV–Visible spectrophotometer (Cecil CE 3021, Cambridge, England).

2.10. Thymol loading and release

Chitosan hydrogels were incubated in thymol hydroalcoholic solutions (2.5 mg·mL^{-1} and 1.25 mg·mL^{-1}) for 7 h. The hydrogels were washed with water and after that 1 mL of phosphate buffered saline (PBS) or modified Fusayama Meyer artificial saliva (NaCl 6.8 mM, KCl 5.4 mM, $CaCl_2$ 5.4 mM, Na_2HPO_4 1.6 mM, urea 16 mM) (AS) was added in the top of each gel to perform the release assay. The release medium was removed at different time points from the hydrogels and replenish with fresh media. The cumulative thymol release was measured through the Folin-Ciocalteau spectrophotometeric method, widely used to determine polyphenols and phenols content. Briefly, 200 μL of supernatant from each hydrogel were mixed with 200 μL of phenol reagent and 2 mL of Na_2CO_3 (2% w/v) solution. After 1 h incubation with the reagents, each sample was measured at 725 nm in a UV–VIS Spectrophotometer (Cecil CE 3021, Cambridge, England).

2.11. Bacterial cell viability test

2.11.1. MTT assay and SEM analysis

Chitosan hydrogels were incubated in anaerobiosis at 37 °C in Todd-Hewitt 5% glucose broth with 1×10^6 CFU of *Streptococcus mutans*. After 24 h, in some hydrogels MTT reagent was added (5 mg·mL^{-1} in PBS). *Streptococcus mutans* reduces MTT dye (3-(4,5-dimetylthiazol-2-yl)-2,5-diphenyl-tetrazolium bromide) into insoluble purple formazan. These chitosan hydrogels were dissolved in acetic acid 1% (v/v) and subsequent dilutions in ethanol were performed. The coloured solutions due to the dissolution of formazan crystals were measured at 570 nm in a UV-VIS Spectrophotometer. (Cecil CE 3021, Cambridge, England). In parallel, hydrogels were fixed and analysed by scanning electron microscopy (SEM) as described in Section 2.3.

2.12. Antimicrobial activity test

2.12.1. Plate count method

A bacterial suspension of 1.10^6 CFU·mL^{-1} in PBS or AS was added to chitosan and thymol-loaded chitosan hydrogels. The hydrogels were incubated overnight at 37 °C. After 24 h, the bacterial suspension on the top of the hydrogels was withdrawn and serial dilutions were made in physiologic solution from each supernatant. Finally, 20 μL of each solution was spread in agar plates and the number of colony forming units was counted.

This methodology was repeated two more times, to evaluate the sustained antimicrobial effect of the synthesized materials after 24 h, 48 h and 72 h. Luria-Bertani (LB) agar plates (yeast extract, 5 g·L^{-1}; agar, 15 g·L^{-1}, NaCl, 10 g·L^{-1} and triptone, 10 g·L^{-1}) were used for *Staphylococcus aureus*. While *Streptococcus mutans* was cultured in blood agar plates under anaerobic conditions.

2.13. Antioxidant activity

2.13.1. DPPH assay

The scavenging activity on the stable free radical DPPH was assayed by the modified Blois' method in which the bleaching rate of DPPH is monitored at a characteristic wavelength in presence of the sample [52]. The assay was performed as follows: 100 μL supernatants of chitosan and thymol-loaded chitosan hydrogels were mixed with 400 μL of Tris buffer pH = 7.4 and 500 μL DPPH 100 μM. Absorbance was measured at 517 nm. DPPH inhibition was calculated by the equation:

$$\%\text{inhibition} = [1 - (A_{sample}/A_{DPPH\ solution})] \times 100$$

where A is the absorbance measured.

2.13.2. Simil peroxidase activity

Thymol-chitosan hydrogels simil peroxidase activity was also performed by the method described by Herzog and Fahimi [53]. After their synthesis and incubation, 200 μL of the hydrogel supernatants were mixed with 25 μL H_2O_2 0.030 M and 775 μL diaminobencidine tetrahidrochloride (DAB) 1.10^{-4} M prepared in Krebs-Henseleit buffer (pH: 7.4) containing: 125 mM NaCl; 4.0 mM KCl; 0.5 mM NaH_2PO_4; 0.1 mM $MgCl_2$; 1.1 mM $CaCl_2$ and 5.0 mM glucose. A DAB solution without H_2O_2 was used as reaction blank. The reaction was initiated by the addition of H_2O_2 and the change in OD readings was recorded at 30 s intervals for 5 min using a Shimadzu recording spectrophotometer UV-240 (graphic printer PR-1) set at 465 nm. Then the Δ absorbance/min was calculated. A calibration curve of peroxidase concentration *vs* Δ absorbance/min was plotted using horseradish peroxidase of known

concentration, obtaining a linear relationship in the range of 1.95×10^{-3} to 2.5×10^{-5} U·mL^{-1}. The activity of samples was calculated by interpolation in the standard curve.

2.13.3. Simil superoxide dismutase activity

The simil superoxide dismutase activity was determined by the capacity to inhibit epinephrine auto-oxidation, to adrenochrome, in presence of atmosphere oxygen [54]. For this purpose, 50 μL of the hydrogel supernatant, 910 μL phosphate buffer pH = 10.7 and 40 μL 2 mM epinephrine were mixed. The resulting absorbance was measured at 480 nm every 10 s for 5 min. Δ absorbance/min was calculated. The antioxidant activity of samples was evaluated as the % of epinephrine auto-oxidation inhibition by the following equation:

$$\%\text{inhibition} = [(\Delta\text{Abs}/\text{min}_{\text{epinephrine}} - \Delta\text{Abs}/\text{min}_{\text{sample}})/\Delta\text{Abs}/\text{min}_{\text{epinephrine}}] \times 100$$

2.14. Statistical analysis

Data are represented as means ± SD of at least triplicate experiments. For some data, the differences were analysed by ANOVA (analysis of variance), followed by a Bonferroni multiple comparison test. For some other data, Student's *t*-test was performed. In every statistical evaluation $p < 0.05$ was considered significant.

3. Results and discussion

3.1. Chitosan hydrogels synthesis and characterization

Chitosan hydrogels were synthesized by a spraying method. The fast neutralization of chitosan multicationic chains was achieved by the application of a sodium hydroxide 0.1 M spray, which promotes an immediate gelation. The preparation of chitosan hydrogels by this technique guarantees a porous structure and a high surface area which are highly desirable properties to enhance cell adhesion and proliferation into the matrix while improving drug incorporation. The homogeneous polymer network, pore structure and approximate pore size were observed by scanning electron microscopy (SEM) and transmission electron microscopy (TEM) (Fig. 1).

In addition, Fourier transform infrared spectrum (FTIR) showed a peak at 1550 cm^{-1} corresponding to(−N−H−) bending peak and an amide I peak at 1650 cm^{-1} (C═O). There was also a broad band at 3500–3100 cm^{-1} that could be attributed to (N−H) and (O−H) stretching vibrations. FTIR spectrum is consistent to chitosan with a high degree of deacetylation [34] (Fig. 2a).

Differential scanning calorimetry analysis is a technique widely used for polymer characterization which has the capacity to determine physical and chemical changes in biopolymers like chitosan. In the DSC thermogram (Fig. 2b), a characteristic endothermic peak at 126.7 °C was observed, which can be attributed to the loss of water [55]. This result implies that there is a fraction of non-freezing water present in the hydrogel and it is closely associated with the polysaccharide matrix [56,57]. Consequently, chitosan hydrogel DSC curve is consistent with its swelling behavior.

Swelling studies were performed in thymol-chitosan hydrogels (Fig. 3a). Chitosan and thymol-loaded chitosan hydrogels showed good swelling properties, they absorbed a high amount of water and the swelling process followed a second order kinetics (Fig. 3b). Hydrogel swelling profile reveals that almost in 1 h the swelling ratio reached equilibrium. In Table 1, chitosan hydrogels and thymol-chitosan hydrogels water content at equilibrium are detailed reaching up to ~96% of water (Table 1). It is worth to mention that hydrogels which have high water content show good permeability and biocompatibility being clear advantages for medical applications [58].

Additionally, rheological studies indicated that chitosan was an elastic dominantly hydrogel, because the storage modulus G′ values (*ca.* 1000 Pa) were always greater than the loss modulus (*ca.* 100 Pa) G″ values [59] (Fig. 2c). Elastic dominantly hydrogels usually have good swelling behavior. Therefore, chitosan hydrogels viscoelastic properties agree with its swelling profile.

In brief, viscoelastic properties, swelling performance and DSC results indicate that chitosan hydrogels have a strong affinity for water, encouraging the mucoadhesion of chitosan to the oral mucosa. Indeed, water represents almost 95% of the mucous layer weight.

Chitosan biodegradability was also evaluated. Especially because saliva is a fluid which contains several electrolytes and proteins like lysozyme, that is capable to degrade chitosan as it can hydrolyze β-1,4 bonds between *N*-acetylmuramic acid and *N*-acetyl-D-glucosamine monomers. After 7 days of incubation, thymol-loaded chitosan hydrogels were degraded by lysozyme (Fig. 3c).

3.2. Chitosan hydrogels biocompatibility studies and thymol release studies

Once chitosan hydrogels were characterized, cytocompatibility assays with [3T3] fibroblasts were prepared. Fibroblasts are usually found in connective tissue. They are responsible for the synthesis of collagen, glycoaminoglycans and other extracellular matrix components. Therefore, they have an important role in soft tissue regeneration. The MTT results showed that hydrogels are cytocompatible for at least 24 h, so they are feasible to be used as scaffolds. The number of viable cells seeded on the chitosan hydrogels increased approximately 4 times after 24 h. ($p < 0.05$) (Fig. 4).

Due to its high degree of deacetylation, chitosan is mainly composed of glucosamine residues exhibiting a great amount of amine and

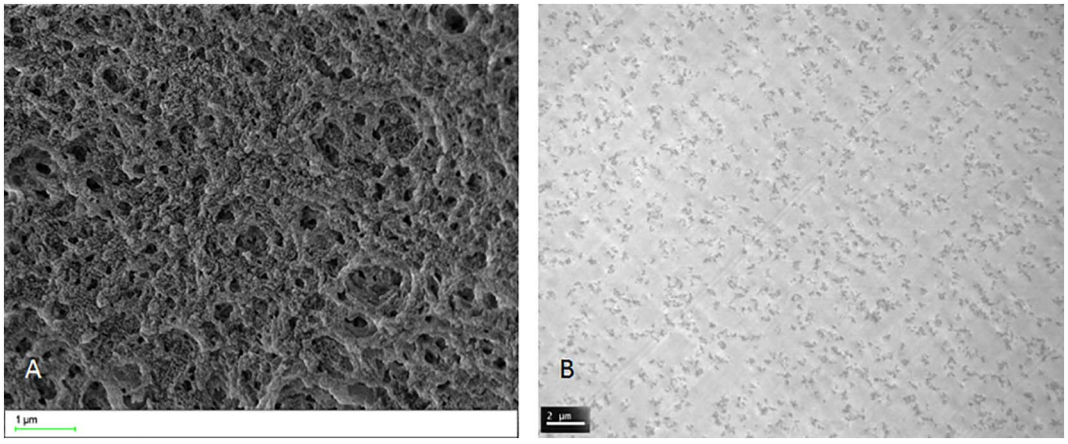

Fig. 1. (A) Representative scanning electron microscopy image of chitosan hydrogel (B) representative transmission electron microscopy image of chitosan hydrogel.

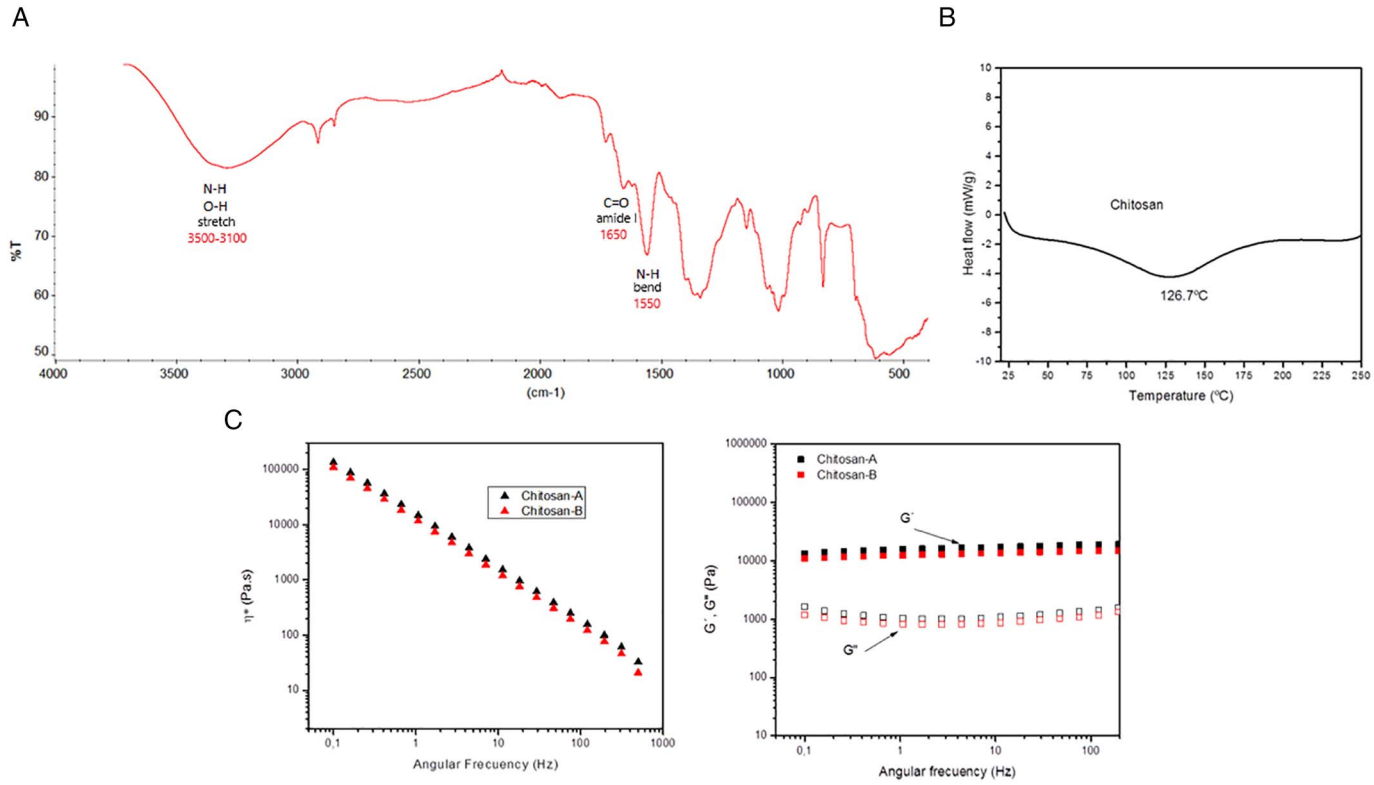

Fig. 2. (A) Fourier transform infrared spectrum from lyophilized chitosan hydrogel (B) chitosan hydrogel differential scanning calorimetry thermogram at a heating rate of 10 °C·min^{-1} under a nitrogen flow of 50 mL·min^{-1} (C) Complex viscosity of chitosan hydrogel against frequency - Viscoelastic response of chitosan hydrogel against frequency (G′ and G″). (n = 2).

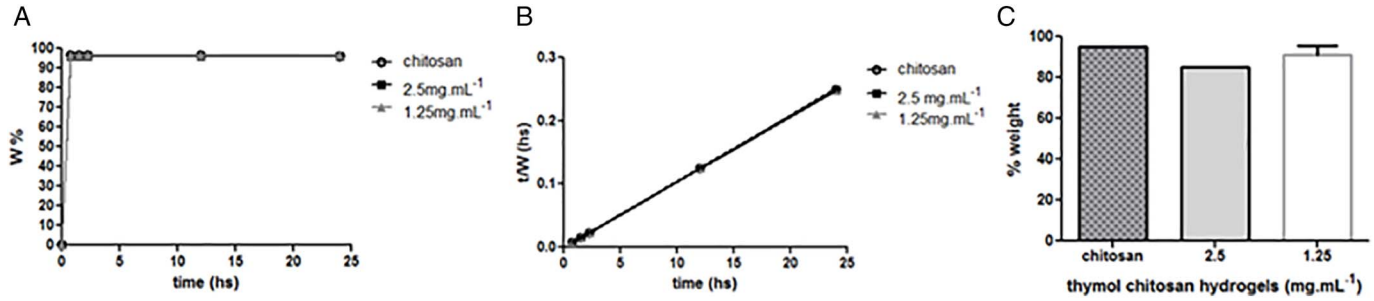

Fig. 3. (A) Degree of swelling of chitosan and thymol-chitosan hydrogel over a period of 24 h in phosphate-buffered saline (n = 6) (B) chitosan and thymol-chitosan hydrogel experimental data of water content and time plotted according to a second order kinetic (n = 6) (C) biodegradation of thymol-chitosan hydrogels in a period of 7 days with 1 mg·mL^{-1} of lysozyme in phosphate-buffered saline.

Table 1
Chitosan and thymol-chitosan hydrogels water content at equilibrium (W_∞) and coefficient of determination (r^2) of water content and time plotted according to a second order kinetic.

	r^2	W_∞
Chitosan	0.9998	96.12
2.5 mg·mL^{-1}	0.9998	96.25
1.25 mg·mL^{-1}	0.9999	96.62

hydroxyl groups which are available for the formation of hydrogen bonds and electrostatic interactions with thymol phenol group. Thus, it could be hypothesized that thymol can be attached to chitosan by noncovalent bonds, such as electrostatic interactions and hydrogen bonds. Additionally, chitosan hydrogel porosity encourages the proximity between the functional groups leading to the formation of these noncovalent bonds, increasing the incorporation of thymol. Chitosan hydrogels incubated with 2.5 mg·mL^{-1} and 1.25 mg·mL^{-1} thymol solutions incorporated 0.99 ± 0.03 mg of thymol and 0.57 ± 0.03 mg of thymol per hydrogel respectively.

Cumulative thymol release was carried out in two different release media. After 4 h, ~70% of thymol was released in AS media in contrast to PBS, in which the content of thymol released to the media was ~45%. While in phosphate saline buffer, frequently used for *in vitro* drug release measurements to resemble physiologic conditions, 100% of thymol release was achieved in almost 48 h.

In modified Fuyasama Meyer artificial saliva [60], whose composition resembles even more natural saliva, the release of thymol was even faster, reaching almost 100% after 24 h. Nevertheless, both PBS and AS showed similar *in vitro* drug release profiles following a first order release kinetics (Fig. 5). Drug release studies suggest that hydrogels could be used as thymol carriers for an antimicrobial-antioxidant therapy considering its periodic application by the patient in intervals of 2–3 days.

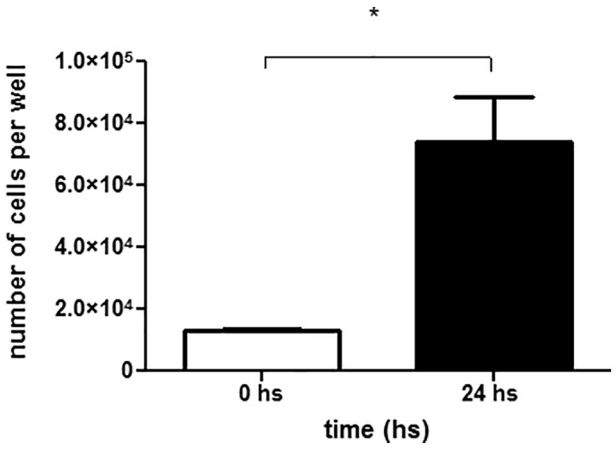

Fig. 4. [3T3] Mouse fibroblast cytocompatibility for 24 h in chitosan hydrogels ($n = 3$) by a colorimetric thiazolyl blue tetrazolium bromide assay for assessing cell proliferation. Absorbance was measured at 570 nm $*p < 0.05$ was considered significant using a Student's *t*-test.

3.3. Chitosan hydrogels bacterial cell viability and antimicrobial activity studies

Literature sustains that chitosan biopolymer has antimicrobial activity. Nevertheless, several factors may have an impact in chitosan behavior. First, we employed a MTT assay to analyse bacterial cell viability cultured in chitosan hydrogels [61] after incubating the hydrogels seeded with bacteria for 24 h in Todd-Hewitt 5% glucose broth. *Streptococcus mutans* viability was significantly higher in chitosan hydrogel blanks than chitosan hydrogels that were incubated with thymol ($p < 0.05$) (Fig. 6d).

In parallel, a scanning electron microscopy analysis was performed to evaluate *Streptococcus mutans* aggregation in chitosan hydrogels with and without thymol after 24 h of incubation in Todd-Hewitt 5% glucose broth. As expected, no bacteria were found in thymol-loaded chitosan hydrogels in contrast with chitosan hydrogels without thymol, which presented high amounts of bacteria attached (Fig. 6b, c). SEM images further confirm that adhesion and aggregation of bacteria were deeply discouraged in thymol-loaded chitosan hydrogels. Results from both techniques support that chitosan hydrogels without thymol are suitable matrices for *Streptococcus mutans* aggregation and proliferation. In contrast to thymol-loaded chitosan hydrogels, in which no aggregation or proliferation was observed.

In the next stage, thymol-chitosan hydrogels antimicrobial activity in PBS and artificial saliva was evaluated. Plate count method was carried out to determine the antimicrobial activity in modified Fusayama Meyer artificial saliva and phosphate saline buffer.

In the chitosan hydrogels without thymol was observed the proliferation of *Staphylococcus aureus* and *Streptococcus mutans* in every reutilization cycle.

The absence of significant antimicrobial activity of unloaded chitosan hydrogels could be attributed to the neutralization of amine groups during gelation process. Chitosan cannot behave as a group of polycationic chains that could be responsible of the antimicrobial activity. Besides, glucosamine groups (pKa ≈ 6.5) are not ionized at physiological pH.

On the contrary, chitosan hydrogels loaded with thymol showed a significant antimicrobial activity against *Staphylococcus aureus* and *Streptococcus mutans* for 3 consecutive reutilization cycles of 24 h when incubated in PBS or AS confirming that thymol- loaded hydrogels present effective antimicrobial activity for 72 h (Fig. 7).

Staphylococcus aureus is a non-oral specie. However, some findings suggest that periodontal microenvironment may establish suitable conditions for the colonization of no members of the oral microbiota in human oral cavity. Indeed, species such as *Pseudomonas aeruginosa* and *Staphylococcus aureus* were found in human subgingival biofilm samples [62]. Otherwise, *Streptococcus mutans* is a facultative anaerobe microorganism, which is part of the oral microbiome. It is strongly related to supragingival plaque. Oral microbiome and dental plaque composition is modulated by several factors, like diet, underlying diseases and tobacco. There is a great inter-individual variability, leading to the administration of broad-spectrum antimicrobials to treat oral diseases, like periodontitis. We analysed antimicrobial activity against two representative types of bacteria, as an illustration of the possible use of thymol-chitosan hydrogels antimicrobial properties against bacteria that could be present in periodontitis patients.

3.4. Chitosan hydrogels antioxidant studies

Finally, we evaluated the antioxidant activity from thymol-chitosan hydrogels. Oxygen reactive species from neutrophils are intended to eradicate pathogens but they could cause irreversible periodontal tissue damage. Irreversible periodontal tissue damage and gingival tissue recession, two main characteristics of periodontal disease, could lead to tooth loss. We performed a DPPH assay and evaluated simil superoxide dismutase and simil peroxidase activity to have a broad panorama of thymol-chitosan hydrogels antioxidant capacities.

Chitosan hydrogels loaded with thymol showed free scavenging capacity by DPPH assay after 24 h in modified Fuyasama Meyer artificial saliva. This method is commonly employed to evaluate antioxidant activity. No significant differences were found in the hydrogels loaded with 0.99 ± 0.03 mg of thymol and 0.57 ± 0.03 mg of thymol ($p < 0.05$).

Simil superoxide dismutase activity and simil peroxidase activity were also analysed. Thymol-chitosan hydrogels showed simil

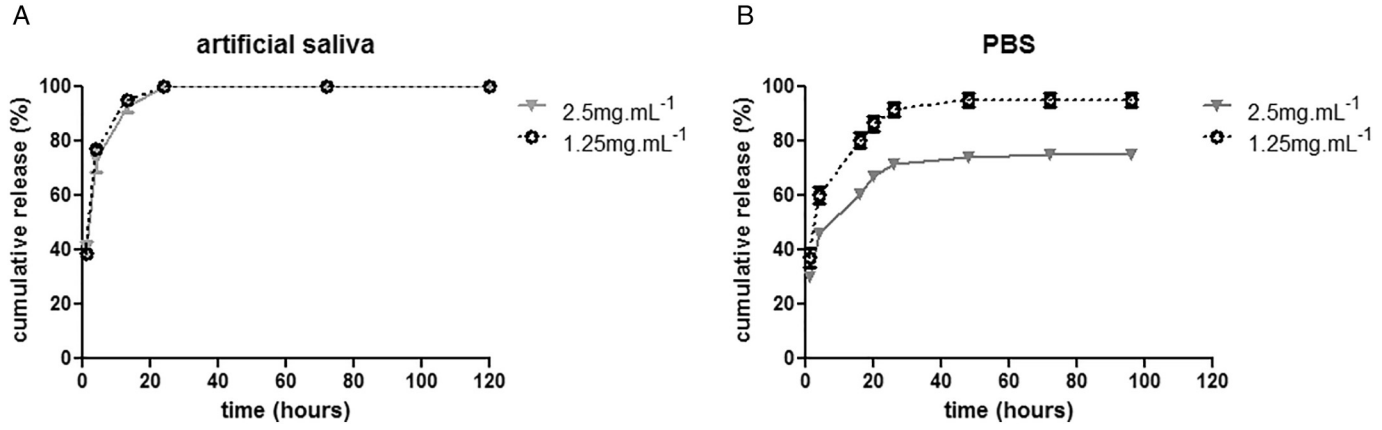

Fig. 5. Cumulative thymol release (A) in artificial saliva and (B) phosphate-buffered saline media from chitosan hydrogels ($n = 3$).

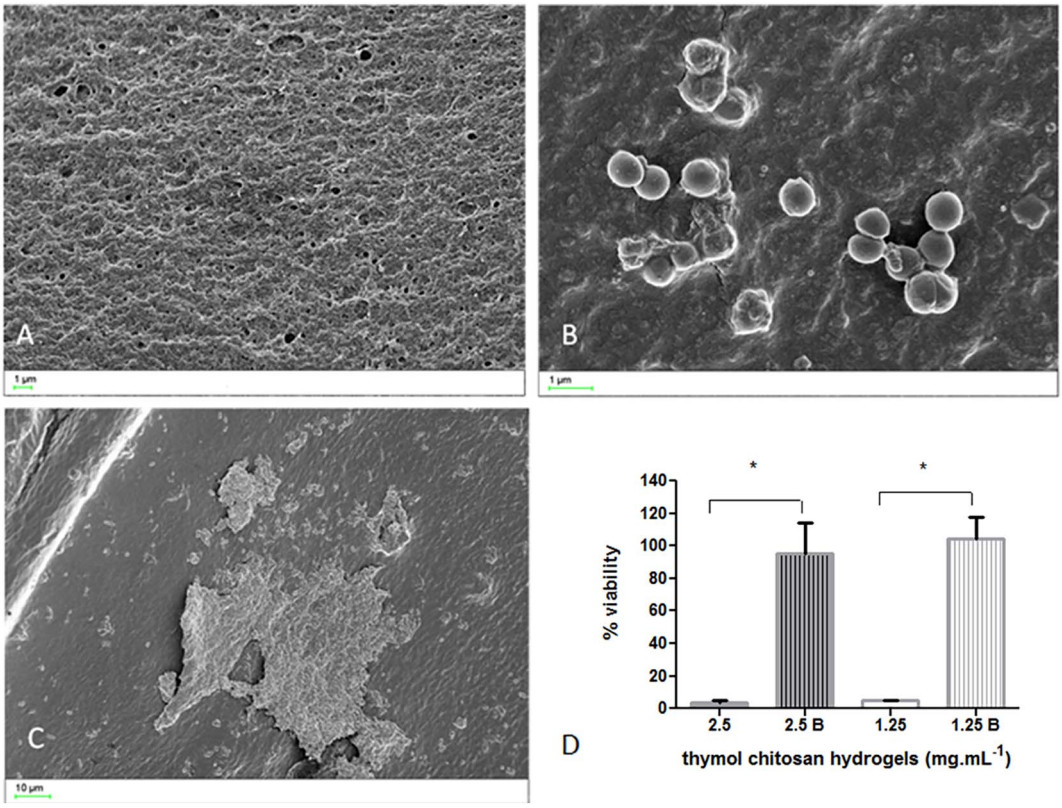

Fig. 6. (A) Scanning electron microscopy image of chitosan hydrogel (B) scanning electron microscopy image of *Streptococcus mutans* on chitosan hydrogel (C) scanning electron microscopy image of *Streptococcus mutans* biofilm on chitosan hydrogel (D) *Streptococcus mutans* viability in thymol-chitosan hydrogels by thiazolyl blue tetrazolium bromide assay after 24 h ($n = 3$). The differences were analysed using one-way ANOVA, followed by Bonferroni multiple comparisons test, $p < 0.05$ was considered significant.

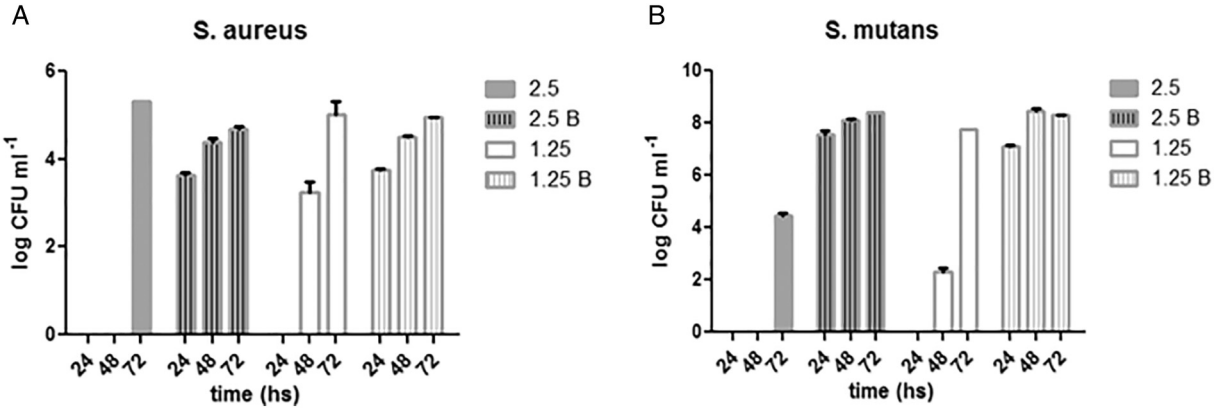

Fig. 7. (A) Thymol-chitosan hydrogels antimicrobial activity *against Staphylococcus aureus* by plate count method over period of 72 h ($n = 3$) (B) thymol-chitosan hydrogels antimicrobial activity against *Streptococcus mutans* by plate count method over period of 72 h ($n = 3$).

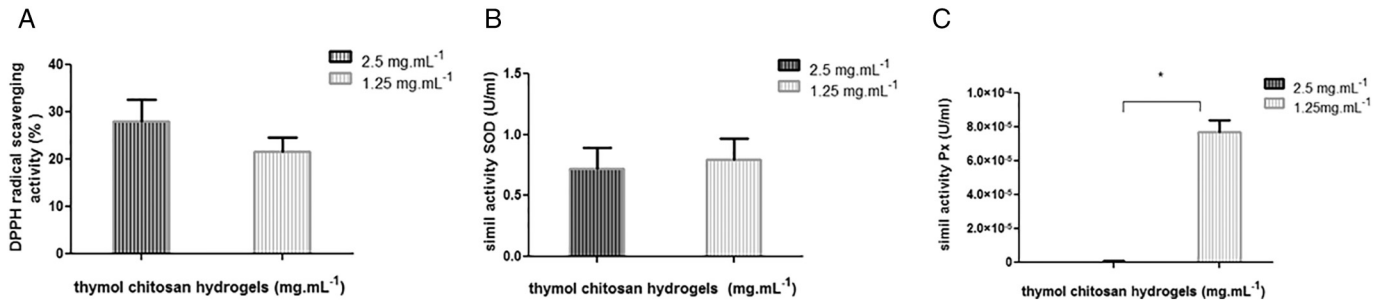

Fig. 8. Thymol-chitosan hydrogels antioxidant activity over a period of 24 h. (A) α, α-diphenyl-β-picrylhydrazyl radical scavenging activity (B) simil activity peroxidase (C) simil activity superoxide dismutase. Results are expressed as mean ± SEM of three determinations performed in triplicate. *$p < 0.05$ was considered significant using a Student's *t*-test.

superoxide dismutase activity. It was observed that they could inhibit epinephrine oxidation at pH = 10.7 proving the ability to scavenge superoxide anion, from atmosphere oxygen. However, chitosan hydrogels showed simil peroxidase activity only when they were loaded with 0.57 ± 0.03 mg of thymol. ($p < 0.05$). Surprisingly, thymol-chitosan hydrogels with the lower amount of thymol presented scavenging activity as well as simil superoxide dismutase and simil peroxide activity (Fig. 8).

The antioxidant activity exerted by the lower amount of thymol could protect the alveolar bone and connective tissue from inflammation injury induced by the oxidative stress generated during periodontitis. As well, free radicals and reactive oxygen species (ROS) are essential to many normal biologic processes, at low concentrations. However, at higher concentrations it may result in tissue injury.

4. Conclusions

Oral health provides quality of life [63]. Most people have dental cavities and several factors such as smoking, lack of oral hygiene and genetics promote the development of oral diseases that might end in tooth loss.

Chitosan hydrogels exemplify a possible delivery system for a dual therapy of periodontitis. In one hand, thymol antioxidant properties would be able to decrease periodontal inflammation; on the other hand, thymol could be an adjuvant of mechanical plaque control because of its antimicrobial activity. Although dental plaque elimination decreases patient inflammation signs, inflammation treatment should be included in gingivoperiodontal therapy.

Thymol-chitosan hydrogels presented antimicrobial activity against *Staphylococcus aureus* and *Streptococcus mutans* for 72 h. Indeed, no adhesion or aggregation of *Streptococcus mutans* was observed in thymol-loaded chitosan hydrogels in a period of 24 h. Not only is relevant to develop a material that releases an antimicrobial, it is also important to prevent the material to be colonized by bacteria [64,65] and also preserve its biocompatibility [66].

Although a burst release was observed within the first 48 h, chitosan hydrogels can be easy administrated and several applications in the mucosa could be done if necessary. In addition, they showed good cytocompatibility, which is particularly important because the oral mucosa is sensible to irritant substances.

The chitosan hydrogels prepared in the present study were fully characterized. Viscoelastic properties, swelling behavior and thermal analysis were pointed out to show chitosan strong affinity for water, promoting its mucoadhesion to the oral mucosa.

In conclusion, *in vitro* results indicate that thymol-chitosan hydrogels may have two different objectives, to treat dental biofilm and adverse consequences of inflammation. Further *in vivo* studies are in course.

Conflict of interest

The authors report no conflict of interest.

Acknowledgements

M. I. Alvarez Echazú is grateful for her doctoral fellowship granted by Universidad de Buenos Aires. The authors would like to acknowledge the support of grants from the Universidad de Buenos Aires UBACYT 20020150100056BA, from CONICET PIP 11220120100657CO and from Agencia Nacional de Investigaciones Cientificas y Técnicas PICT 2012-1441 and PICT 2015-2922 (to M. F. D).

References

[1] Q. Gan, J. Zhu, Y. Yuan, H. Liu, J. Qian, Y. Li, C. Liu, A dual-delivery system of pH-responsive chitosan-functionalized mesoporous silica nanoparticles bearing BMP-2 and dexamethasone for enhanced bone regeneration, J. Mater. Chem. B 3 (2014) 2056–2066.
[2] A.M. Mebert, C. Aime, G.S. Alvarez, Y. Shi, S.A. Flor, S.E. Lucangioli, M.F. Desimone, T. Coradin, Silica core-shell particles for the dual delivery of gentamicin and rifamycin antibiotics, J. Mater. Chem. B 4 (2016) 3135–3144.
[3] N. Tabary, F. Chai, N. Blanchemain, C. Neut, L. Pauchet, S. Bertini, E. Delcourt-Debruyne, H.F. Hildebrand, B. Martel, A chlorhexidine-loaded biodegradable cellulosic device for periodontal pockets treatment, Acta Biomater. 10 (2014) 318–329.
[4] C. Hélary, M.F. Desimone, Recent advances in biomaterials for tissue engineering and controlled drug delivery, Curr. Pharm. Biotechnol. 16 (2015) 635–645.
[5] M.D.S. Silva, N.L. Neto, S.A. da Costa, S.M. da Costa, T.M. Oliveira, R.C.D. Oliveira, M.A.A.M. Machado, Biophysical and biological characterization of intraoral multilayer membranes as potential carriers: a new drug delivery system for dentistry, Mater Sci Eng C Mater Biol Appl 71 (2017) 498–503.
[6] W. Pichayakorn, P. Boonme, Evaluation of cross-linked chitosan microparticles containing metronidazole for periodontitis treatment, Mater Sci Eng C Mater Biol Appl 33 (2013) 1197–1202.
[7] C. Dhand, M. Venkatesh, V.A. Barathi, S. Harini, S. Bairagi, E. Goh Tze Leng, N. Muruganandham, K.Z.W. Low, M.H.U.T. Fazil, X.J. Loh, D.K. Srinivasan, S.P. Liu, R.W. Beuerman, N.K. Verma, S. Ramakrishna, R. Lakshminarayanan, Bio-inspired crosslinking and matrix-drug interactions for advanced wound dressings with long-term antimicrobial activity, Biomaterials 138 (2017) 153–168.
[8] N.R. Johnson, Y. Wang, Drug delivery systems for wound healing, Curr. Pharm. Biotechnol. 16 (2015) 621–629.
[9] R. Lakshminarayanan, R. Sridhar, X.J. Loh, M. Nandhakumar, V.A. Barathi, M. Kalaipriya, J.L. Kwan, S.P. Liu, R.W. Beuerman, S. Ramakrishna, Interaction of gelatin with polyenes modulates antifungal activity and biocompatibility of electrospun fiber mats, Int. J. Nanomedicine 9 (2014) 2439–2458.
[10] R. Lakshminarayanan, V.A. Barathi, M. Venkatesh, N.K. Verma, S. Liu, X.J. Loh, R.W. Beuerman, Membrane Selectivity of Cationic Polyamides and Rational Design of Proteolytic-resistant Antimicrobial Peptides Investigative Ophthalmology & Visual Science, 57 (2016), p. 333.
[11] M.V. Thomas, D.A. Puleo, Infection, inflammation, and bone regeneration: a paradoxical relationship, J. Dent. Res. 90 (2011) 1052–1061.
[12] G. Hajishengallis, The inflammophilic character of the periodontitis-associated microbiota, Mol Oral Microbiol 29 (2014) 248–257.
[13] S.C. Sundararaj, M.V. Thomas, R. Peyyala, T.D. Dziubla, D.A. Puleo, Design of a Multiple Drug Delivery System Directed at Periodontitis Biomaterials, 34 (2013), pp. 8835–8842.
[14] A. Leszczynska, P. Buczko, W. Buczko, M. Pietruska, Periodontal pharmacotherapy - an updated review, Adv. Med. Sci. 56 (2011) 123–131.
[15] S. Petti, C. Scully, Polyphenols, oral health and disease: a review, J. Dent. 37 (2009) 413–423.
[16] N. Tamaki, R. Cristina Orihuela-Campos, Y. Inagaki, M. Fukui, T. Nagata, H.-O. Ito, Resveratrol improves oxidative stress and prevents the progression of periodontitis via the activation of the Sirt1/AMPK and the Nrf2/antioxidant defense pathways in a rat periodontitis model, Free Radic. Biol. Med. 75 (2014) 222–229.
[17] F.W.M.G. Muniz, S.B. Nogueira, F.L.V. Mendes, R. Kuchenbecker, M.M.S.M. Moreira, G.M. de Andrade, R.D.S. Carvalho, The impact of antioxidant agents complimentary to periodontal therapy on oxidative stress and periodontal outcomes: a systematic review, Arch. Oral Biol. 60 (2015) 1203–1214.
[18] T. Maruyama, T. Tomofuji, Y. Endo, K. Irie, T. Azuma, D. Ekuni, N. Tamaki, T. Yamamoto, M. Morita, Supplementation of green tea catechins in dentifrices suppresses gingival oxidative stress and periodontal inflammation, Arch. Oral Biol. 56 (2011) 48–53.
[19] A. Leszczynska, P. Buczko, W. Buczko, M. Pietruska, Periodontal pharmacotherapy an updated review, Adv. Med. Sci. 56 (2011) 123–131.
[20] C.J. Smiley, S.L. Tracy, E. Abt, B.S. Michalowicz, M.T. John, J. Gunsolley, C.M. Cobb, J. Rossmann, S.K. Harrel, J.L. Forrest, P.P. Hujoel, K.W. Noraian, H. Greenwell, J. Frantsve-Hawley, C. Estrich, N. Hanson, Systematic review and meta-analysis on the nonsurgical treatment of chronic periodontitis by means of scaling and root planing with or without adjuncts, J. Am. Dent. Assoc. 146 (2015) 508-524.e505.
[21] S.M. Nabavi, A. Marchese, M. Izadi, V. Curti, M. Daglia, S.F. Nabavi, Plants belonging to the genus *Thymus* as antibacterial agents: from farm to pharmacy, Food Chem. 173 (2015) 339–347.
[22] A. Marchese, I.E. Orhan, M. Daglia, R. Barbieri, A. Di Lorenzo, S.F. Nabavi, O. Gortzi, M. Izadi, S.M. Nabavi, Antibacterial and antifungal activities of thymol: a brief review of the literature, Food Chem. 210 (2016) 402–414.
[23] R. Gyawali, S.A. Ibrahim, Natural products as antimicrobial agents, Food Control 46 (2014) 412–429.
[24] M.E. Embuscado, Spices and herbs: Natural sources of antioxidants - a mini review, J. Funct. Foods 18 (Part B) (2015) 811–819.
[25] J. Lizardi-Mendoza, W.M. Arguelles Monal, F.M. Goycoolea Valencia, G. Romanazzi, A. Jimenez-Aparicio, Chapter 1 - chemical characteristics and functional properties of chitosan A2, in: Silvia Bautista-Banos, G. Romanazzi, A. Jiménez-Aparicio (Eds.), Chitosan in the Preservation of Agricultural Commodities, Academic Press, San Diego, 2016, pp. 3–31.
[26] T. Jiang, R. James, S.G. Kumbar, C.T. Laurencin, Chapter 5 - Chitosan as a Biomaterial: Structure, Properties, and Applications in Tissue Engineering and Drug Delivery, Natural Synthetic Biomed Polym, Elsevier, Oxford, 2014, pp. 91–113.
[27] B. Fonseca-Santos, M. Chorilli, An overview of carboxymethyl derivatives of chitosan: Their use as biomaterials and drug delivery systems, Mater Sci Eng C Mater Biol Appl (2017), http://dx.doi.org/10.1016/j.msec.2017.1003.1198.

[28] A. Aljawish, I. Chevalot, J. Jasniewski, J. Scher, L. Muniglia, Enzymatic synthesis of chitosan derivatives and their potential applications, J. Mol. Catal. B Enzym. 112 (2015) 25–39.
[29] E.M. Costa, S. Silva, C. Pina, F.K. Tavaria, M.M. Pintado, Evaluation and insights into chitosan antimicrobial activity against anaerobic oral pathogens, Anaerobe 18 (2012) 305–309.
[30] W.A. Sarhan, H.M.E. Azzazy, High concentration honey chitosan electrospun nanofibers: biocompatibility and antibacterial effects, Carbohydr. Polym. 122 (2015) 135–143.
[31] X.J. Loh, Latest advances in antibacterial materials, J. Molec. Eng. Mat. 5 (2017) 1740001.
[32] M. Hosseinnejad, S.M. Jafari, Evaluation of different factors affecting antimicrobial properties of chitosan, Int. J. Biol. Macromol. 85 (2016) 467–475.
[33] L. Zhao, Y. Hu, D. Xu, K. Cai, Surface functionalization of titanium substrates with chitosan-lauric acid conjugate to enhance osteoblasts functions and inhibit bacteria adhesion, Colloids Surf. B Biointerfaces 119 (2014) 115–125.
[34] X. He, K. Li, R. Xing, S. Liu, L. Hu, P. Li, The production of fully deacetylated chitosan by compression method Egyptian, J. Aquat. Res. Educ. 42 (2016) 75–81.
[35] X. Li, Z. Yang, A. Zhang, The effect of neurotrophin-3/chitosan carriers on the proliferation and differentiation of neural stem cells, Biomaterials 30 (2009) 4978–4985.
[36] J.D. Bumgardner, V.P. Murali, H. Su, O.D. Jenkins, D. Velasquez-Pulgarin, J.A. Jennings, A. Sivashanmugam, R. Jayakumar, 4 - Characterization of chitosan matters, Chitosan Based Biomaterials Volume 1, Woodhead Publishing, 2017, pp. 81–114.
[37] S. Ahmed, S. Ikram, Chitosan based scaffolds and their applications in wound healing, Achiev. Life Sci. 10 (2016) 27–37.
[38] P. Manivasagan, J. Oh, Marine polysaccharide-based nanomaterials as a novel source of nanobiotechnological applications, Int. J. Biol. Macromol. 82 (2016) 315–327.
[39] R. Zafar, K.M. Zia, S. Tabasum, F. Jabeen, A. Noreen, M. Zuber, Polysaccharide based bionanocomposites, properties and applications: a review, Int. J. Biol. Macromol. 92 (2016) 1012–1024.
[40] N. Jain, G.K. Jain, S. Javed, Z. Iqbal, S. Talegaonkar, F.J. Ahmad, R.K. Khar, Recent approaches for the treatment of periodontitis, Drug Discov. Today 13 (2008) 932–943.
[41] N. Mati-Baouche, P.-H. Elchinger, H. de Baynast, G. Pierre, C. Delattre, P. Michaud, Chitosan as an adhesive, Eur. Polym. J. 60 (2014) 198–212.
[42] W. Kanjanakawinkul, T. Rades, S. Puttipipatkhachorn, T. Pongjanyakul, Nicotine-magnesium aluminum silicate microparticle surface modified with chitosan for mucosal delivery, Mater Sci Eng C Mater Biol Appl 33 (2013) 1727–1736.
[43] E. Russo, F. Selmin, S. Baldassari, C.G.M. Gennari, G. Caviglioli, F. Cilurzo, P. Minghetti, B. Parodi, A focus on mucoadhesive polymers and their application in buccal dosage forms, J. Drug Delivery Sci. Technol. 32 (Part B) (2016) 113–125.
[44] A. Pedro, E. Cabral-Albuquerque, D. Ferreira, B. Sarmento, Chitosan: an option for development of essential oil delivery systems for oral cavity care? Carbohydr. Polym. 76 (2009) 501–508.
[45] K. Halake, H.J. Kim, M. Birajdar, B.S. Kim, H. Bae, C. Lee, Y.J. Kim, S. Kim, S. Ahn, S.Y. An, S.H. Jung, J. Lee, Recently developed applications for natural hydrophilic polymers, J. Ind. Eng. Chem. 40 (2016) 16–22.
[46] L. Shue, Z. Yufeng, U. Mony, Biomaterials for periodontal regeneration: a review of ceramics and polymers, Biomatter 2 (2012) 271–277.
[47] Y. Zhou, C. Wu, X. Zhang, P. Han, Y. Xiao, The ionic products from bredigite bioceramics induced cementogenic differentiation of periodontal ligament cells via activation of the Wnt/[small beta]-catenin signalling pathway, J. Mater. Chem. B 1 (2013) 3380–3389.
[48] M.C. Matesanz, J. Linares, I. Lilue, S. Sanchez-Salcedo, M.J. Feito, D. Arcos, M. Vallet-Regi, M.T. Portoles, Nanocrystalline silicon substituted hydroxyapatite effects on osteoclast differentiation and resorptive activity, J. Mater. Chem. B 2 (2014) 2910–2919.
[49] S.B. Qasim, S. Najeeb, R.M. Delaine-Smith, A. Rawlinson, I. Ur Rehman, Potential of electrospun chitosan fibers as a surface layer in functionally graded GTR membrane for periodontal regeneration, Dent. Mater. 33 (2017) 71–83.
[50] T. Momose, H. Miyaji, A. Kato, K. Ogawa, T. Yoshida, E. Nishida, S. Murakami, Y. Kosen, T. Sugaya, M. Kawanami, Collagen hydrogel scaffold and fibroblast growth factor-2 accelerate periodontal healing of class II furcation defects in dog open, Dent. J. 10 (2016) 347–359.
[51] M.I.A. Echazu, M.V. Tuttolomondo, M.L. Foglia, A.M. Mebert, G.S. Alvarez, M.F. Desimone, Advances in collagen, chitosan and silica biomaterials for oral tissue regeneration: from basics to clinical trials, J. Mater. Chem. B 4 (2016) 6913–6929.
[52] M.S. Blois, Antioxidant determinations by the use of a stable free radical, Nature 26 (1958) 1199–1200.
[53] V.H.A.H.D. Fahimi, A new sensitive colori-metric assay for peroxidase using 3,3′diaminobenzidine as hydrogen donors, Anal. Biochem. 55 (1973) 554–562.
[54] H.P. Misra, I. Fridovich, The role of superoxide anion in the autoxidation of epinephrine and a simple assay for superoxide dismutase, J. Biol. Chem. 247 (1972) 3170–3175.
[55] F.S. Kittur, K.V. Harish Prashanth, K. Udaya Sankar, R.N. Tharanathan, Characterization of chitin, chitosan and their carboxymethyl derivatives by differential scanning calorimetry, Carbohydr. Polym. 49 (2002) 185–193.
[56] J. Ratto, T. Hatakeyama, R.B. Blumstein, Differential scanning calorimetry investigation of phase transitions in water/chitosan systems, Polymer 36 (1995) 2915–2919.
[57] L.S. Guinesi, E.T.G. Cavalheiro, The use of DSC curves to determine the acetylation degree of chitin/chitosan samples, Thermochim. Acta 444 (2006) 128–133.
[58] I. Katime, E. Mendizábal, Swelling properties of new hydrogels based on the dimethyl amino ethyl acrylate methyl chloride quaternary salt with acrylic acid and 2-methylene butane-1,4-dioic acid monomers in aqueous solutions, Mater. Sci. Appl. 1 (2010) 162–167.
[59] P. Li, J. Zhao, Y. Chen, B. Cheng, Z. Yu, Y. Zhao, X. Yan, Z. Tong, S. Jin, Preparation and characterization of chitosan physical hydrogels with enhanced mechanical and antibacterial properties, Carbohydr. Polym. 157 (2017) 1383–1392.
[60] M.P. Licausi, A. Igual Muñoz, V. Amigó Borrás, Influence of the fabrication process and fluoride content on the tribocorrosion behaviour of Ti6Al4V biomedical alloy in artificial saliva, J. Mech. Behav. Biomed. Mater. 20 (2013) 137–148.
[61] E. Brambilla, A. Ionescu, A. Mazzoni, M. Cadenaro, M. Gagliani, M. Ferraroni, F. Tay, D. Pashley, L. Breschi, Hydrophilicity of dentin bonding systems influences in vitro Streptococcus mutans biofilm formation, Dent. Mater. 30 (2014) 926–935.
[62] A.P. Vieira Colombo, C.B. Magalhaes, F.A. Hartenbach, R. Martins do Souto, C. Maciel da Silva-Boghossian, Periodontal-disease-associated biofilm: a reservoir for pathogens of medical importance, Microb. Pathog. 94 (2016) 27–34.
[63] J. Durham, H.M. Fraser, G.I. McCracken, K.M. Stone, M.T. John, P.M. Preshaw, Impact of periodontitis on oral health-related quality of life, J. Dent. 41 (2013) 370–376.
[64] X. Zhu, X. Jun Loh, Layer-by-layer assemblies for antibacterial applications, Biomater. Sci. 3 (2015) 1505–1518.
[65] L. Jiang, C.R.R. Gan, J. Gao, X.J. Loh, A perspective on the trends and challenges facing porphyrin-based anti-microbial materials, Small 12 (2016) 3609–3644.
[66] Z. Li, P.L. Chee, C. Owh, R. Lakshminarayanan, X.J. Loh, Safe and efficient membrane permeabilizing polymers based on PLLA for antibacterial applications, RSC Adv. 6 (2016) 28947–28955.